

**LHCb Collaboration**



LHCb-VELO 2007-013

Version 1.0

19th March 2007

---

## VELO Pattern Recognition

**David Hutchcroft**

Department of Physics, University of Liverpool, Liverpool, UK, L69 7ZE

### Abstract

The status of the VELO pattern recognition software for the DC' 06 data production is given. The efficiency for finding tracks with at least 5 GeV/c momentum is 97.4%, with a ghost rate of 6.8%.

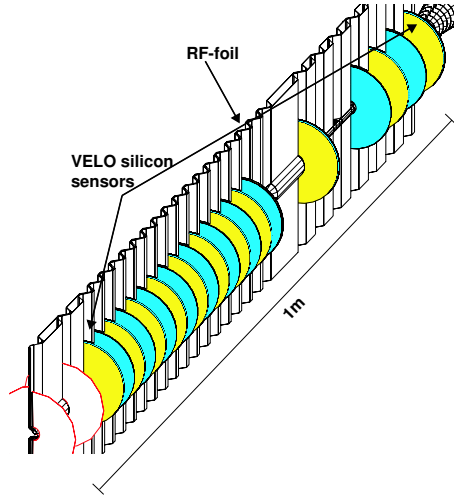


Figure 1: The positions of the sensors from the right hand side of the VELO are shown. The two colours represent the R and Phi sensors, which can be seen alternating down the detector. The two white sensors on the left of the diagram represent the two pileup veto counters. The RF foil is corrugated and allows a small overlap between detector halves in acceptance.

## 1 Introduction

The **Vertex Locator** [1] is a silicon strip detector designed to measure the trajectories of charged particles from the 14 TeV pp collisions delivered by the LHC [2]. LHCb [3, 4] is designed to measure the CP violations in B decays. The design of the detector is driven by three requirements: a good efficiency for reconstructing the B decays, an excellent B lifetime measurement and a trigger capable of rapidly identifying B decays.

The VELO detector consists of 21 stations of silicon detectors. Each station comprises two modules on opposite sides of the detector offset by 15 mm from each other, see figure 1. One module has two detectors, an R detector and a Phi detector, mounted back to back. The R detectors have 2048 strips arranged in four radial sectors of 512 strips each. The strips measure the distance from the nominal  $x=0$ ,  $y=0$  of the sensor of deposited charge, figure 2 shows the R strip layout. The Phi detectors have 2048 strips arranged with a small stereo angle to the local radial direction. They are arranged in two sectors, an inner sector with 683 strips and an outer sector with 1365 strips. The layout of the Phi strips<sup>1</sup> is shown in figure 3.

## 2 Physics requirements

### 2.1 Reconstruction of signal events

The VELO should maximise the number of useful tracks and vertices reconstructed, whilst minimising the amount of material traversed by the tracks. The design of the detector as a single arm spectrometer means that only particles travelling within the forward cone of the LHCb acceptance will have sufficient information to be fully reconstructed. From the nominal interaction point all tracks between 390 mrad and

<sup>1</sup>In this note  $\phi$  denotes the azimuthal angle and Phi refers to the type of sensor.

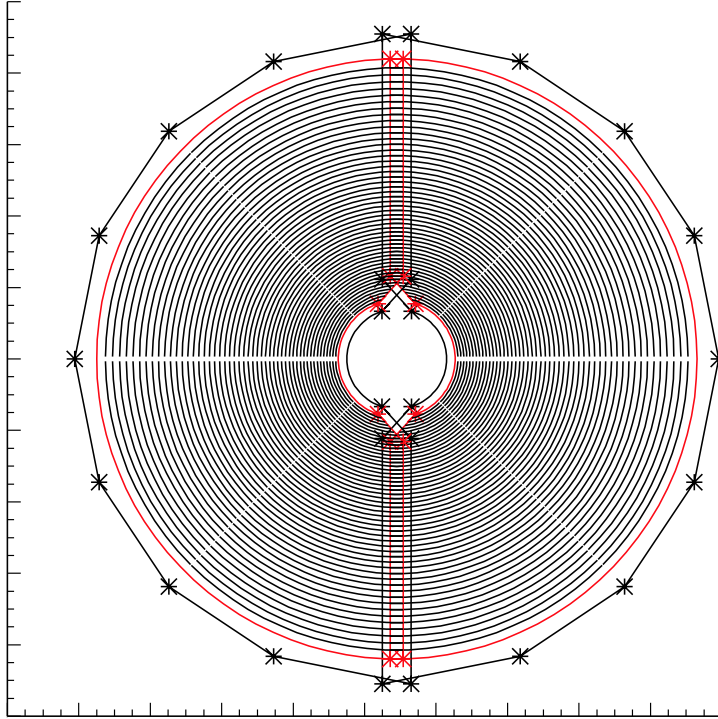


Figure 2: The layout of the R sensor strips showing two sensors on opposite sides of the detector, for clarity only every 10th strip is drawn. The outline of the silicon sensor is marked, as is the outline of the sensitive area of the sensor. The scale has major tick marks at 1 cm intervals.

15 mrad cross at least 3 stations, which is the minimum required to reconstruct the track.

## 2.2 Trigger requirements

The design of the detector was driven by the requirement to provide rapid reconstruction of the tracks for the trigger. In the RZ projection tracks are assumed to be straight lines and using only the R sensor information 2D tracks can be reconstructed and tested to see if they all come from a common vertex, or if some of the tracks are displaced from the interaction point.

## 3 VELO measurements

### 3.1 Strip positions

Each R strip has a nominal radius [5] given by the formulae for the local radius ( $r_i$ ) and pitch ( $P_i$ ):

$$r_i = \frac{\exp(P_{\text{slope}} * i) * P_{\text{inner}} - (P_{\text{inner}} - P_{\text{slope}} * r_{\text{inner}})}{P_{\text{slope}}} \quad (1)$$

$$P_i = \exp(P_{\text{slope}} * i) * P_{\text{inner}} \quad (2)$$

$$P_{\text{slope}} = \frac{P_{\text{outer}} - P_{\text{inner}}}{r_{\text{outer}} - r_{\text{inner}}}. \quad (3)$$

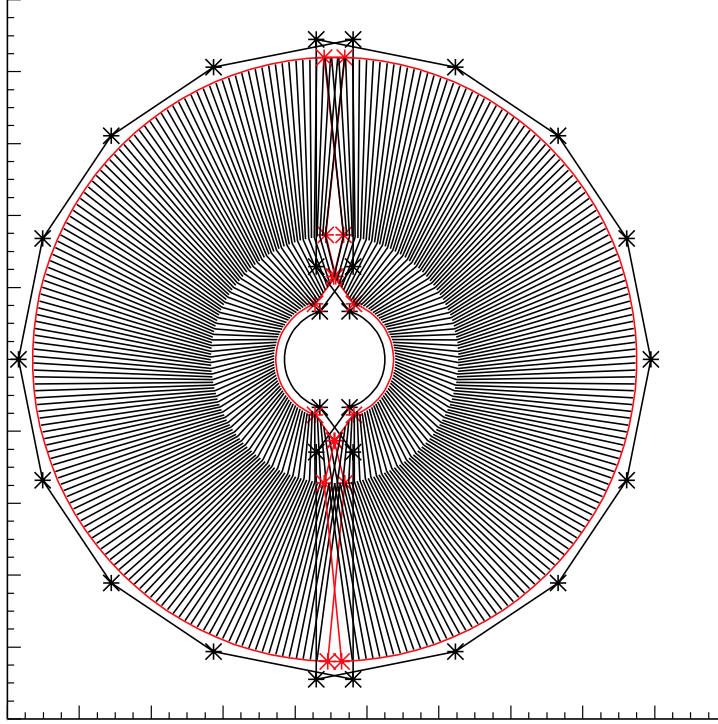


Figure 3: The layout of the Phi sensor strips showing two sensors on opposite sides of the detector, for clarity only every 10th strip is drawn. The outline of the silicon sensor is marked, as is the outline of the sensitive area of the sensor. The scale has major tick marks at 1 cm intervals.

where  $i$  is the number of the strip within a sector (0 to 511),  $r_{\text{inner}} = 7.01$  mm is the inner radius and  $r_{\text{outer}} = 44$  mm the outer radius of the active area of the silicon,  $P_{\text{inner}} = 0.04$  mm and  $P_{\text{outer}} = 0.101553$  mm are the pitches of the inner most and outer most strip in a zone.

For Phi strips the geometry is shown in figure 3. The Phi sensors cover just over  $180^\circ$  in angle and the strips are evenly spaced in the two regions. The inner region runs from  $r = 7.01 - 17.25$  mm and the outer region from  $r = 17.25 - 44$  mm. The strips are arranged so that both inner and outer strips if extended would have a distance of closest approach to the origin of 2.8 mm for the inner region and 3.1 mm for the outer region. The inner and outer regions are skewed in opposite directions to minimise the intrusion into the other half of the detector. If the sensor is at its nominal position then the  $\phi$  of a strip varies along the length with the formula:

$$\phi_i(r) = (i * P_{\text{zone}}) + T_{\text{zone}} - \sin^{-1}(d_0^{\text{zone}}/r) \quad (4)$$

where  $\phi_i(r)$  is the phi of strip  $i$  within a zone at radius  $r$ ,  $d_0^{\text{inner}} = 2.8$  mm,  $d_0^{\text{outer}} = 3.1$  mm,  $T_{\text{inner}} = -1.8750$  radian and  $T_{\text{outer}} = -1.5313$  radian.

### 3.2 Cluster positions

The cluster positions come from the raw output bank [6], which has two sections. The first is a list of strip numbers corresponding to clusters with an inter strip position encoded to a 1/8th strip resolution and a bit indicating if the cluster is bigger than 2 strips. There is also a single bit to indicate a high threshold on the

total ADC count. Using just the strip and fraction of a strip information “light clusters” are created. These light clusters are used in the pattern recognition.

The second section in the raw bank is the list of ADC values for each strip that comprised a cluster. The cluster position can be improved by using a full fit to the ADC values of each strip in a multi-strip cluster. Additional information from the track angle can also be used to improve the cluster position. These full clusters are used in the track fit to give the most precise reconstruction of the track trajectory.

Alignment of the VELO should be very good, the modules at construction are assembled with the R sensors positioned to within  $30\ \mu\text{m}$  of the nominal position. Each R/Phi pair is aligned to within about  $10\ \mu\text{m}$  and about  $0.1\ \text{mrad}$ . Small measured deviations from the nominal positions are corrected by calculating the offsets for groups of strips in advance and applying the corrections when converting clusters from strip numbers to positions.

## 4 Pattern recognition

### 4.1 Two dimensional Pattern Recognition

Each R sector covers just over  $45^\circ$  in azimuth and a straight track from the interaction point should stay within the same sector. The algorithm loops over pairs of modules on the same side of the detector, they are required to be separated by one or two stations. Each combination of one cluster from the first sensor and one from the second sensor is considered. The intersection of the straight line joining the pair of clusters and the intermediate sensor(s) are made. If there is a hit within a small search window the triplet of clusters is retained as a track. The track is then extended in both directions and additional clusters that are close to the projection are added, each updating the trajectory estimate. If the track is in either of the sectors that overlap the detector halves then the hits the appropriate sectors on the other side of the detector are also checked and if compatible added to the track. For further details of the algorithm see [7].

The result of the first stage of the pattern recognition are RZ tracks, these have only R VELO measurements on them, a trajectory in RZ space and an estimate of the azimuth of the track from the  $45^\circ$  sector. These tracks can be used to find 2D vertices and the 2D impact parameter of tracks, which allows the a first check in the trigger to determine if there are any tracks compatible with coming from secondary decays.

### 4.2 Three dimensional Pattern Recognition

The three dimensional pattern recognition starts from the RZ tracks found in the two dimensional pattern recognition and attempts to add the Phi clusters to the tracks. It does this by taking all clusters from the sensors compatible with the RZ track, also allowing the track to be extended by one additional station in either direction. It uses the sensor furthest from the interaction point and works toward the interaction region. From the Phi sensors only clusters that are compatible with the RZ track  $\phi$  range are considered. The  $\phi$  of the cluster is calculated by using the  $r$  estimate from the RZ track at the  $z$  of the sensor. A second Phi cluster is added from the next station and from that a full 3D trajectory is made. The track is then extended by adding more clusters that are sufficiently close to the extrapolated trajectory. At least three Phi clusters are required to have been attached to the track candidate and also that more than a required fraction of stations had hits.

More than one 3D track might be compatible with an RZ track, and each possibility is created simultaneously. At the end of the track extension the choice between

track candidates is made based on the length of the track in Phi clusters found and in the event of a tie in  $\chi^2$ . There may also be track candidates which have several common clusters, in this case the lists are merged and a combined longer track is created.

## 5 Fitting tracks in the VELO

VELO clusters represent either an arc or a line in 3D space with an associated error that the track is supposed to have passed through. For the purposes of the pattern recognition the lack of any knowledge of the momentum means the assumed multiple scattering can be significant on the scale of the strip pitch. The 2D and 3D trajectories in the pattern recognition are built by assuming the R and Phi sensor clusters represent measurements of  $r$  and  $\phi$  (after correction for radius). For the final track fit [9, 11] based on the Kalman filter [10] the full 3D position of the sensors with known misalignments is used.

As part of the RZ pattern recognition a linear fit to the clusters is performed, this is used primarily as a best estimator of the track  $r$  at a given  $z$ . For the 3D pattern recognition a 3D fit is performed with both R and Phi clusters. The fit starts by averaging the  $\phi$  coordinate of the clusters on the track to define a frame. The R and Phi clusters are used to fit the  $u$  and  $v$  stereo coordinates where  $u$  is the radial axis and  $v$  is the axis perpendicular to  $u$  resolved at the average  $\phi$ . The errors in both cases come from the `VeloCoord` objects which use  $N \cdot \text{pitch} / \sqrt{12}$  for  $N$  strip clusters. An additional term `MSStep` is introduced to de-weight clusters through each station, this accumulates as the track moves away from the smallest  $r$  value. This improves the estimate of the track position extrapolated to the vertex by de-weighting clusters that were produced after the track passed through material and so multiple scattered from its initial trajectory. Tracks with a  $\chi^2/ndf$  of greater than 4.0 are rejected.

## 6 Performance

### 6.1 Code version uses in tests

The code is based on Brunel version 31r0. The events used are about 10k generic B events generated with spillover and pileup at  $2 \cdot 10^{32} \text{ cm}^2 \text{ s}^{-1}$  from the standard DC' 06 sample [8].

The versions of the relevant packages and default options for this version of Brunel are listed in appendix A.

### 6.2 Pattern recognition efficiency

The pattern recognition for the normal data taking is optimised for the tracks originating from B decays that can be fully reconstructed in the detector. The minimum number of hits required to find the track within the VELO is three R and three Phi hits. The LHCb detector is not hermetic and the acceptance is approximately  $2.1 < \eta < 4.9$  in the  $+z$  direction. Unless otherwise quoted the acceptance criteria for MC particles was defined as the MC Particle had:

- $2.1 < \eta < 4.9$
- $p > 1 \text{ GeV}/c$
- Number of R clusters  $\geq 3$
- Number of Phi clusters  $\geq 3$

- Production vertex radius  $< 0.1$  mm

The overall 3D pattern recognition efficiency was 96.5%, with an event weighted efficiency<sup>2</sup> of 96.8%. This varies significantly as a function of momentum and production radius but is stable in  $z$ : see figure 4 for the plots. The more stringent selection often quoted is that a MC particle be not an electron, with enough hits to create a long track and more than 5 GeV/c momentum; the efficiency for this selection is 97.4%.

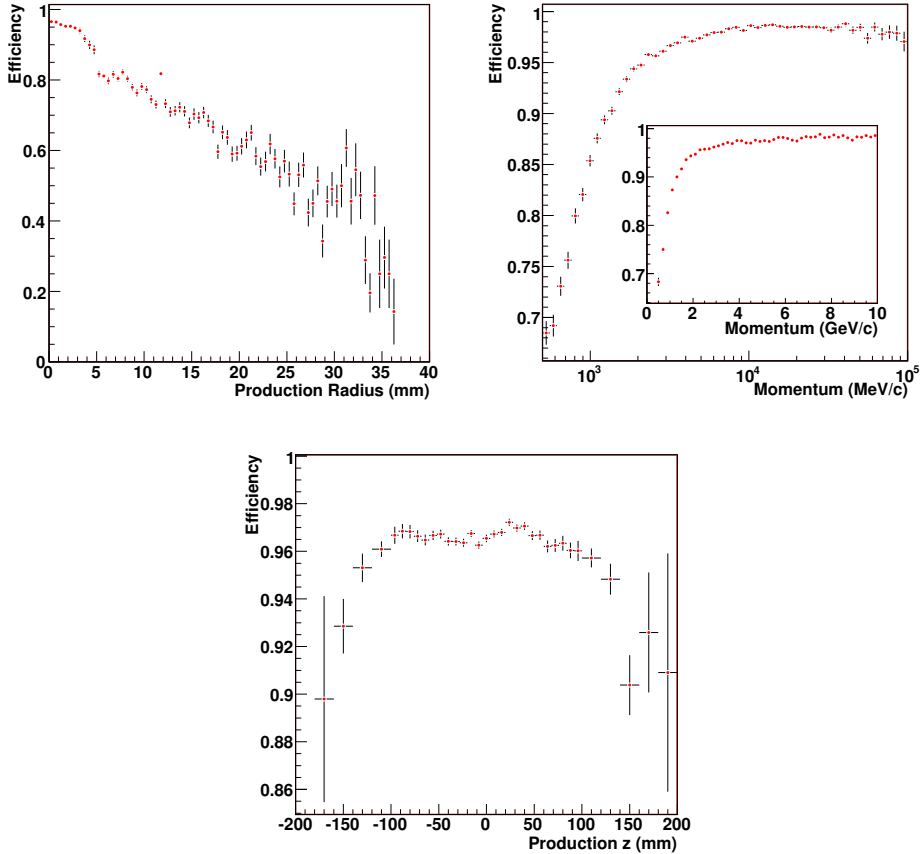


Figure 4: Efficiency plots for the 3D pattern recognition. Top Left: As a function of the production radius of the track; Top Right: As a function of the momentum (inset on linear scale); Bottom: As a function of the production vertex in  $z$  [Note suppressed zero on some scales].

The efficiency is not 100% primarily as the search windows for finding compatible clusters are restricted. For example to make the initial R cluster triplet the separation of the track extrapolation and the cluster centre must differ by less than  $0.9 \times P_i$ , where  $P_i$  is the local strip pitch. Hence the search window varies from  $36 - -91 \mu\text{m}$  depending on the radius of the track at the sensor. The search window to add additional R clusters is a less stringent  $3.5 \times P_i$ . This reduces the number of random combinations, but on tracks with multiple scattering can mean the track does not remain inside the search windows. For a 1 GeV/c  $\pi^+$  passing through both silicon sensors in a station there will be a scatter with a width of of about

<sup>2</sup>The event weight is the average of the quantity calculated separately for each event.

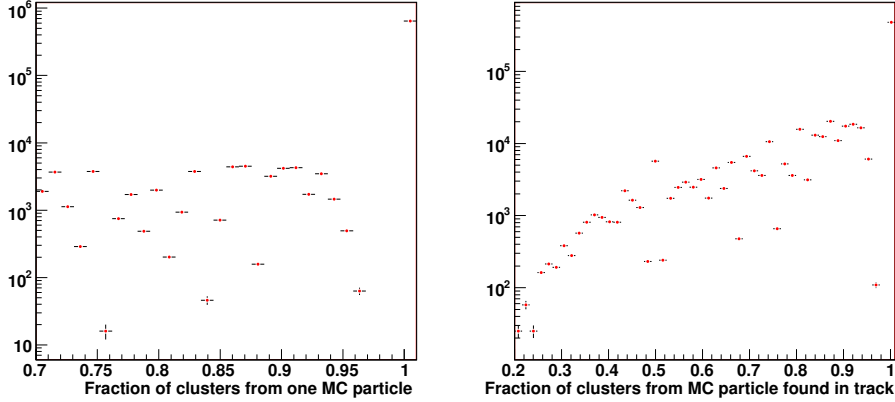


Figure 5: Left: The fraction of clusters for tracks matched to MC truth coming from one MC particle [Note: in 93% of tracks all clusters come from the same MC particle]. Right: The fraction of clusters created by the MC particle found by the pattern recognition in tracks matched to MC truth [Note: in 69% of tracks all MC clusters are found]. The large apparent bin to bin scatter in both plots is caused by the integer division of numbers of clusters.

1 mrad [12], giving a deviation of about  $27 \mu\text{m}$  over the 3 cm to the next station. These deviations are within the normal search windows, however in 2% of multiple scatters the track scatters by significantly more than the core Gaussian.

The efficiency drop as a function of radius is caused by two effects. First the number of sensors crossed by the track is fewer which implies the probability of finding three aligned R and Phi clusters is smaller. Second to reduce ghosts the RZ and 3D tracks are required to point roughly at the interaction point. The opening angle for secondary decays can mean the cluster combinations are projected to have large impact parameters and pass closest to the beam axis at a large negative  $z$  for forward tracks.

In tracks with more than 70% of clusters from one MC particle the average fraction is that 98.9% of clusters come from that MC particle, rising to 99.3% for  $> 5 \text{ GeV}/c$  tracks from B decays. The fraction of clusters created by a MC particle found by the pattern recognition is 93.4%, rising to 97.4% for  $> 5 \text{ GeV}/c$  tracks from B decays, see figure 5.

There is a small rate (0.6%) of tracks that have two MC particles associated to the hits that created them. These are 97% from electron positron pairs created from a photon conversion in the material of the RF foil or the sensors. The two electrons can be produced with an almost identical energy and momentum and deposit energy in the same clusters in the VELO.

A ghost is defined as any track that when the MC truth is examined had less than 70% of the clusters from any one MC particle. Figure 6 shows the number of clusters used in the production of tracks and the number seen in ghost tracks. Also shown in that figure is the relative number of clusters created by the MC when a track is found or not. The overall ghost rate is 6.8%, with the event weighted average 4.7%. The bias that tracks tend to have slightly more R clusters than Phi clusters is due to the requirement to find tracks based on the R clusters alone as the initial stage.

Ghost tracks are predominately shorter, particularly in the number of R clusters, larger  $\chi^2/ndf$  and at lower  $\eta$  than the correctly reconstructed tracks, see figure 7.



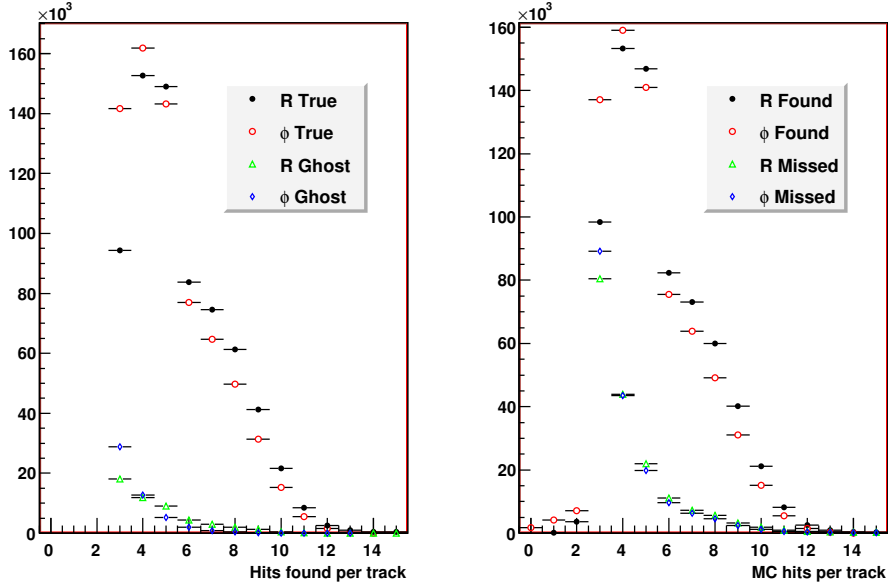


Figure 6: Left: The number of clusters found on tracks matched to MC truth and for ghost tracks for R and Phi clusters separately. Right: The number of clusters created by MC tracks for the tracks found in the pattern recognition and missed by the pattern recognition

A pair of cloned track is where the pattern recognition created two (or more) tracks both of which can be matched to the same MC particle. The clone rate is 2.2%, when event weighted is 1.5%, for tracks matched to MC particles satisfying the above criteria.

Figure 8 shows the number of common R and Phi clusters for the clone tracks. The clones are generally caused either by a significant multiple scatter in one station or by the discontinuity in the sensor separation. In the downstream direction the VELO extends further from the interaction region to cover the LHCb acceptance. Fewer sensors are required to ensure at least 3 stations are crossed by each track, see fig. 8. Tracks crossing this region need to be extrapolated further and sometimes leads to the track position in RZ being outside the cluster search window in the next station.

Tracks are also reconstructed outside the nominal acceptance of the LHCb detector. Figure 10 shows the  $\eta$  distribution of reconstructed tracks and for all MC tracks of at least 0.5 GeV/c that produced at least three R and three Phi clusters.

Table 1 lists the standard performance metrics for the 2D and 3D VELO pattern recognition.

## 7 Non standard conditions

### 7.1 VELO open tracking

At the beginning of a fill the VELO will be operated in an open configuration. The diagram in figure 11 shows the acceptance in the  $(\eta, \phi)$  plane for the fully open (3cm), half open (1.5cm) and closed VELO. For this arrangement of the sensors the

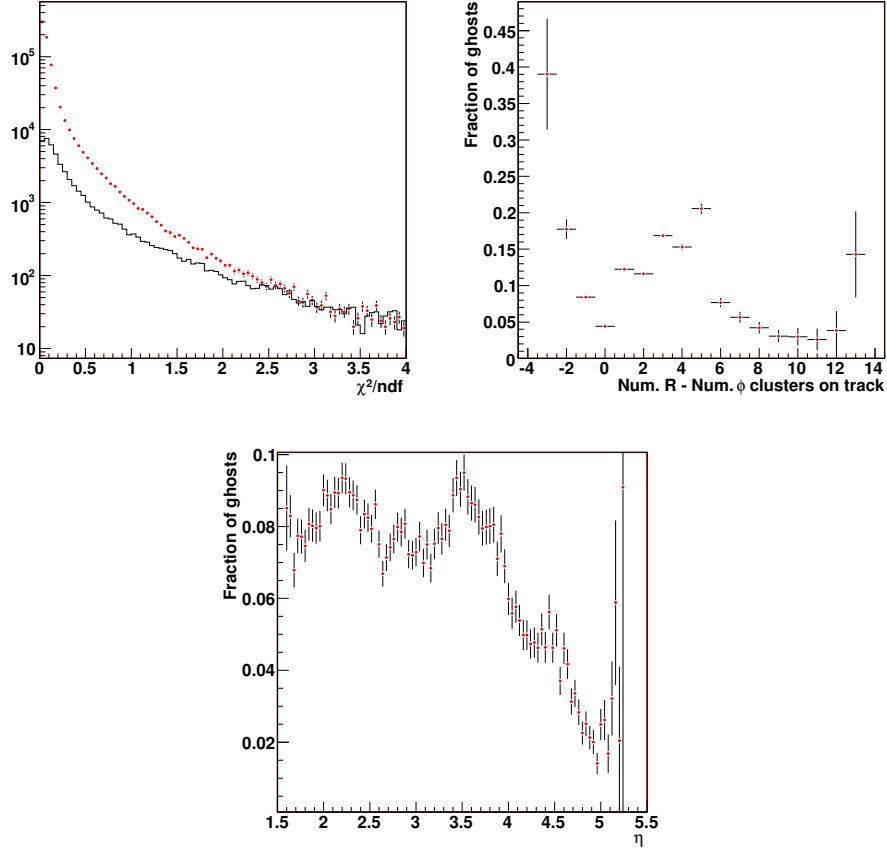


Figure 7: Top Left: The  $\chi^2/ndf$  of the true (points) and ghost (line) tracks. Top Right: The fraction of ghost tracks as a function of difference between number of R and Phi clusters on tracks. Lower: The ghost rate as a function of  $\eta$ .

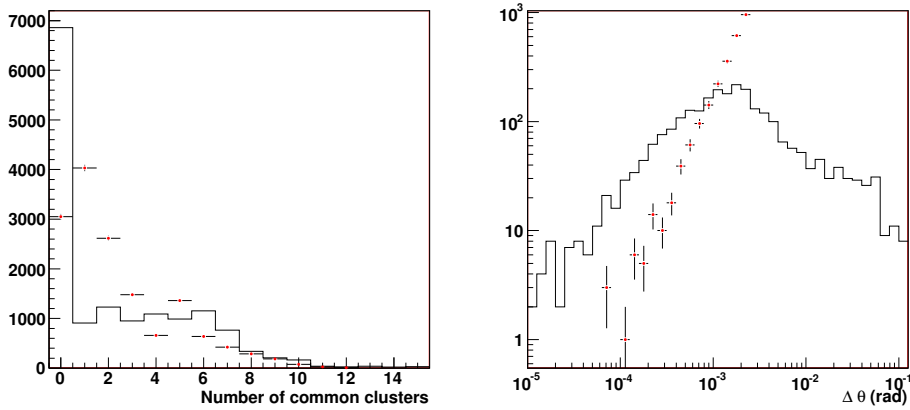


Figure 8: Left: Plot of the number of common clusters in clone tracks for R (line) and Phi (points). Right: Plot of the angle between pair of clone tracks (line) and all combinations of a non-clone tracks (points) where one track is correctly matched to a MC particle.

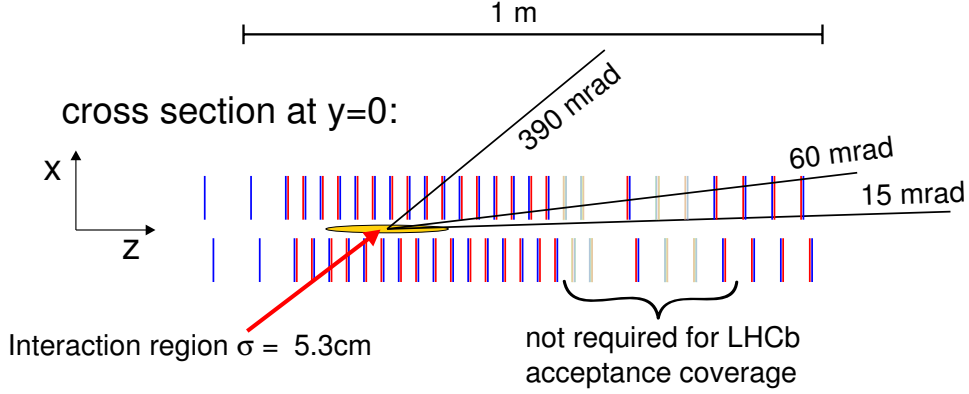


Figure 9: Diagram of the VELO sensor layout in the RZ plane. The pale sensors were removed during the LHCb re-optimisation.

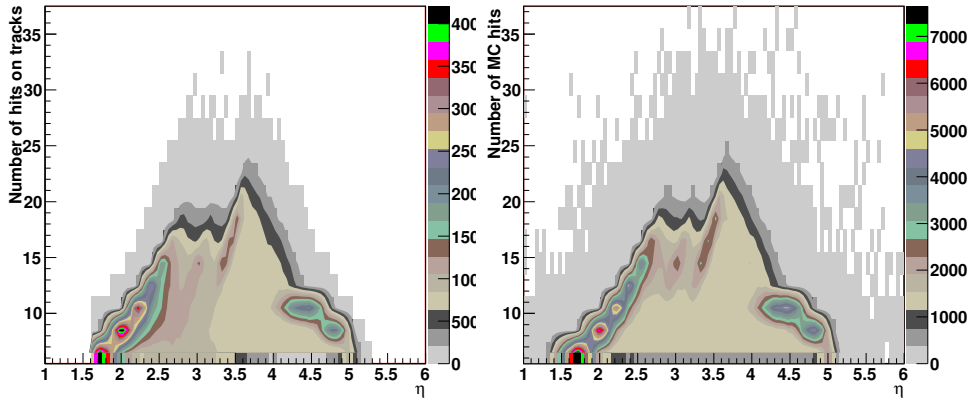


Figure 10: Left: The number of clusters found on tracks verse  $\eta$ . Right: The number of clusters created by MC tracks verse  $\eta$ . Each bin on the vertical scale is two units high, as in general a track will have an even number of clusters due to the close pairing of R and Phi sensors.

	Long tracks	Long $p > 5 \text{ GeV}$	s-Daughters Long	s-Daughters Long $p > 5 \text{ GeV}$	Ghost Evt.	Time (ms)
Setup						0.587
2D	98.0 %	98.9 %	89.0 %	92.1 %	6.8 %	0.659
3D	95.6 %	97.4 %	79.6 %	85.7 %	4.7 %	2.441

Table 1: Performance on 10k events at  $\mathcal{L} = 2 \times 10^{32} \text{cm}^2 \text{s}^{-1}$ . Listed are the efficiencies, Ghost Evt. is the event weighted ghost rate and the amount of user time spent per event on average. s-Daughters are the tracks coming from decays of hadrons containing  $s$  quarks where the parent was created at  $r < 8 \text{ mm}$  and the daughter tracks pass the long track criteria. The setup line refers to the time taken in PatInitEvent, DecodeVeloRawBuffer and PatVeloLoadClusters.

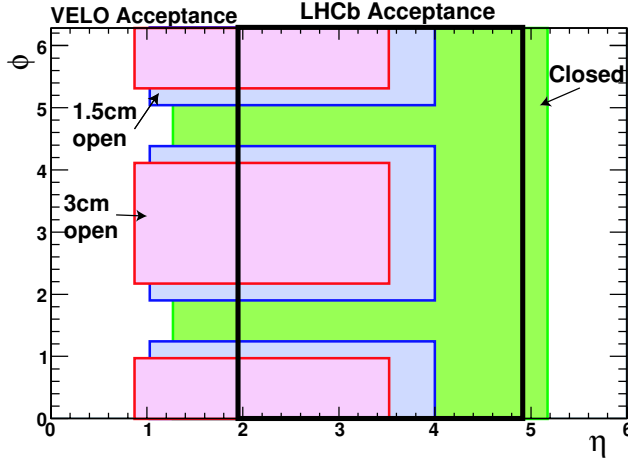


Figure 11: The acceptance of the VELO detector for tracks to cross three stations in the closed, half-open and fully open case.

assumption that the tracks do not cross R-sensors is incorrect. Both the 2D and 3D parts of the tracking can also look for tracks crossing between R sectors. In fact only tracks crossing from the upper and lower sectors<sup>3</sup> in R to the sectors closest to  $x=0$  as the track increases in radius are searched for.

To implement this change two additional options must be set in the code, see appendix A.2, these reduce the efficiency and increase the ghost rate if used when the detector is in its nominal position.

## 7.2 Pilot run conditions

	Long tracks	Long Trk. $p > 5 \text{ GeV}$	Ghost Evt.	Time (ms)
Setup				0.262
2D	92.6%	96.3%	2.2%	0.064
3D	84.3%	88.7%	0.3%	0.058

Table 2: Pattern recognition performance for minimum bias events in pilot run conditions with the VELO fully open. Listed are the efficiencies, Ghost Evt. is the event weighted ghost rate and the amount of user time spent per event on average. The setup line refers to the time taken in PatInitEvent, DecodeVeloRawBuffer and PatVeloLoadClusters.

Table 2 shows the efficiencies for events simulating the running conditions of the pilot run. The events are 5k of minimum bias with the VELO fully open; each side retracted by 3 cm. With the default cuts the efficiencies for 3D tracking are below 40% per track.

## 7.3 High luminosity running

Table 3 shows the efficiencies for generic B events simulating the high luminosity conditions ( $\mathcal{L} = 5 \times 10^{32} \text{ cm}^2 \text{ s}^{-1}$ ). The efficiency is similar, although the ghost rate

<sup>3</sup>Upper and lower in this case refer to the two sectors closest to the vertical axis in the coordinates of the local gravitation field frame.

	Long tracks	Long $p > 5$ GeV	s-Daughters Long	s-Daughters Long $p > 5$ GeV	Ghost Evt.	Time (ms)
Setup						0.629
2D	97.8 %	98.7 %	87.9 %	91.6 %	15.1 %	1.035
3D	95.2 %	97.0 %	77.7 %	84.5 %	9.0 %	3.353

Table 3: Performance on 10k events at  $\mathcal{L} = 5 \times 10^{32} \text{cm}^2 \text{s}^{-1}$ . Listed are the efficiencies, Ghost Evt. is the event weighted ghost rate and the amount of user time spent per event on average. s-Daughters are the tracks coming from decays of hadrons containing  $s$  quarks where the parent was created at  $r < 8$  mm and the daughter tracks pass the long track criteria. The setup line refers to the time taken in PatInitEvent, DecodeVeloRawBuffer and PatVeloLoadClusters.

has approximately doubled and the code takes about 40 % longer to run. This is expected from the increased number of cluster combinations to resolve within an event.

## 8 Plans to tune software with real data

The first tests of the code have been performed with the VELO test beam data taken in 2007 with five modules from the final detector operational. The number of modules that could be read out concurrently was limited by the availability of the readout systems. Pseudo-efficiencies for the tracking were produced where a module was deliberately removed from the pattern recognition. Tracking was performed normally in the other modules and the area around the track impact point was examined for the presence of clusters, see figure 12. The average distance from the track to the cluster (if one is present) can be used to set the cluster search window size.

The same analysis will be performed with the full detector and the profile of clusters close to the track extrapolations will allow the tuning of the search windows in the VELO pattern recognition.

An estimate of the efficiency could be obtained by reconstructing all but one track from a multi-track  $B$  vertex. For example  $B^+ \rightarrow J/\psi K^+ \pi^+ \pi^-$  which is a 5 track  $B$  vertex with a branching ratio of 0.001. When the  $J/\psi$  decays to two muons the event should pass the L0 and HLT  $J/\psi(\mu\mu)$  streams and if two of the other tracks are reconstructed should be written out into the normal output. Using a TT-T station track identified as a  $\pi$  or  $K$  the “missing” track parameters can be reconstructed from the position of the secondary vertex and the momentum estimate from the TT to T station step. Tight cuts on the  $B^+$  mass will reduce the number of fake combinations. The efficiency for muons and electrons can be estimated in a similar manner using the same decays but comparing rates of events reconstructed in the trigger and those passing through other trigger streams.

The efficiency should be estimated both as a function of the particle type and for both charges separately as this is a systematic error on the CP asymmetry of decays.

The ghost rate can only be estimated from MC events. The efficiency and noise rates for the sensors will be measured and reproduced, while the tuned proton PDFs should allow a reasonable description of the track density and so cluster density for minimum bias events. Then comparing the distributions of  $\chi^2/ndf$  etc. between data and MC, then using these to further tune the MC to match the data.

The clone rate can be assessed by reconstructing narrow resonances (e.g.  $J/\psi$

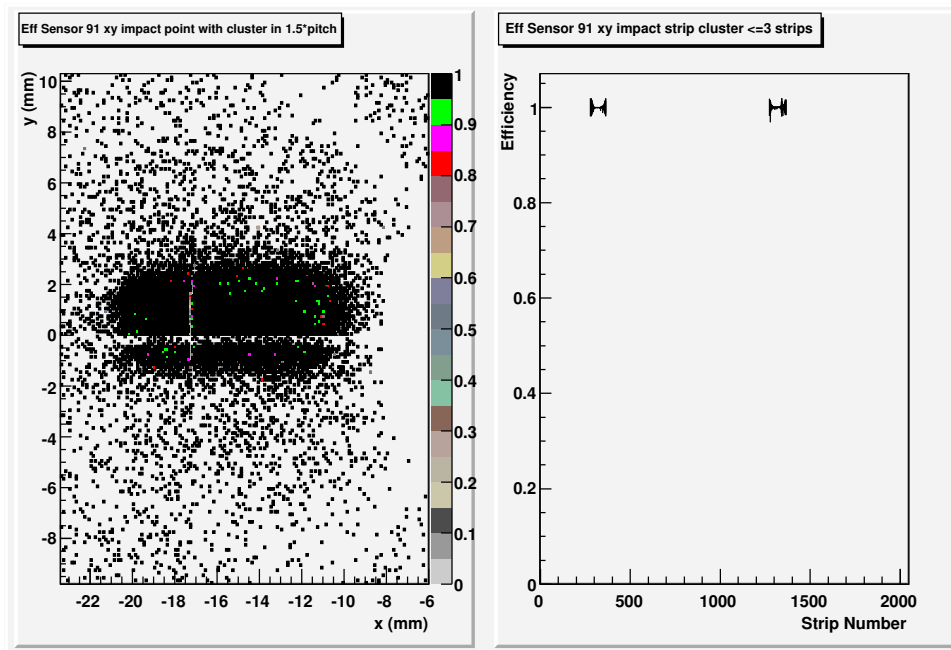


Figure 12: Left: The pseudo-efficiency map for sensor number 91, a Phi sensor, for tracks created without sensor 91 or the paired R sensor if there is a strip within 1.5 x the local strip pitch. The gap at  $y=0$  is due to the insensitive region in the R sensors at that point. Right: The efficiency as a function of strip number if a cluster is within 3x local strip pitch of the track, the two areas shown correspond to the strips in the inner and outer regions crossed by the beam profile.

or  $K_s^0$ ) with more than one VELO track matched to a track in the T stations. If either of the VELO tracks can be used to make the same resonance then they are almost certainly to be clones.

## 9 Conclusions

In the DC'06 Monte Carlo data the VELO pattern recognition provides a good efficiency of around 97.4% for high momentum tracks that cross the whole detector, and a fake rate of around 4.7%. This data was generated with a perfectly aligned detector, but with a higher dead channel rate and more noise than is expected for the initial running of the VELO.

Adding an additional stage to improve the efficiency for tracks produced at higher radius is required.

## A Appendix: Brunel Setup

These tests were run in Brunel v31r0 using the PatVelo v2r10 version of the VELO pattern recognition<sup>4</sup>. The VELO open tracking for the pilot run data used the newer version of the code: PatVelo v2r11, see section A.2. The input files are part of the standard production of DC'06 data, except for the Pilot run data which was private production of events with the same code versions.

<sup>4</sup>The VELO pattern recognition is unchanged from the Brunel version used in DC'06[8]

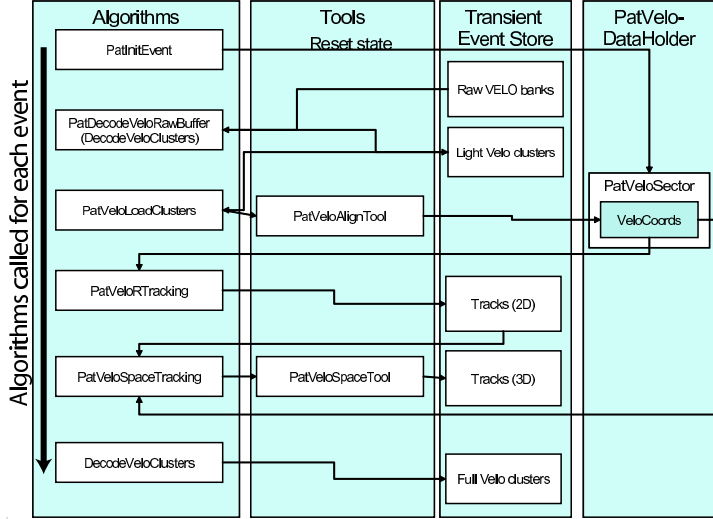


Figure 13: Flow of information through the sequence of algorithms to do pattern recognition in the VELO in Brunel.

Algorithm	User Time (ms)
PatInitEvent	0.042
DecodeVeloRawBuffer	0.115
PatVeloLoadClusters	0.421
PatVeloRTracking	0.659
PatVeloSpaceTracking	2.441
DecodeVeloClusters	1.107

Table 4: Time taken in each algorithm for the nominal luminosity ( $\mathcal{L} = 2 \times 10^{32} \text{cm}^2 \text{s}^{-1}$ ), the time is the average spent in the algorithm. These numbers are only indicative as they were made on a batch node that would have also been running other jobs and are scaled by the apparent speed of the computer, which varies by up to 50%.

The execution of the algorithms and tools is shown in figure 13.

The algorithms are `PatInitEvent` which resets the tool `PatVeloDataHolder` to empty the sectors of clusters, `DecodeVeloRawBuffer` which decodes the raw buffers to make light VELO clusters on the transient event store (TES). Next is `PatVeloLoadClusters` which converts light clusters to `VeloCoord` which have the  $r$  or  $\phi$  calculated and are sorted and stored in `PatVeloSectors` which correspond to each quarter of an R sensor or the inner or outer region of a Phi sensor. The tool `PatVeloAlignTool` applies the small corrections for known misalignment to the  $r$  and  $\phi$  of the sensors. `PatVeloRTracking` is the algorithm that finds 2D RZ tracks, `PatVeloSpaceTracking` and the associated tool `PatVeloSpaceTool` adds the Phi clusters to the RZ tracks. Finally `DecodeVeloClusters` is another instance of `DecodeVeloRawBuffer` which decodes to full VELO clusters for the subsequent track fits. Table 4 lists the time taken in each of the algorithms, except for `DecodeVeloClusters` each is necessary for the subsequent processing.

## A.1 DC'06 tune of the code

The code has several tunable parameters for different conditions, these are the default settings for DC'06.

### PatVeloRTracking

- ZVertexMin = -180 mm** Track projects to a larger  $z$  than this at  $r = 0$ .
- MaxRSlope = 0.400** Slope in  $RZ$  projection must be smaller than this, applies both to forward and backward tracks.
- rMatchTol = 0.90** When creating initial triplets the additional fraction of the local strip pitch a cluster, including error, can be from the projected track.
- rExtraTol = 3.5** After the triplet is created the additional fraction of the local strip pitch a cluster, including error, can be from the projected track.
- rOverlapTol = 0.6** The additional fraction of the local strip pitch a cluster, including error, can be from the projected track when adding clusters from the other side of the VELO.
- MaxMissed = 3** The maximum number of sensors that the projection of the track should pass through that did not register a cluster.
- MinToTag = 4** To prevent reuse of clusters in different tracks they can be tagged as used. This sets the minimum number of clusters found on an R-track to trigger this process for this track.
- AdjacentSectors = false** Turn off the search for clusters crossing sectors.

### PatVeloSpaceTracking

- stepError = 0.002** Estimate of the multiple scattering error caused by each station for the 3D track fit.
- MaxChiSq = 4.0** Maximum  $\chi^2/ndf$  for a track to be accepted.
- CleanOverlaps = true** Remove R clusters on the opposite side of the detector from tracks that are not reconstructed in the  $\phi$  of the overlap region.

### PatVeloSpaceTool

- MarkClustersUsed = true** Mark clusters as used as they are added to tracks.
- FractionFound = 0.35** Minimum fraction of sensors that have clusters on the track for a track to be accepted.
- PhiAngularTol = 0.005** Additional range in  $\phi$  to search for Phi cluster to match the  $RZ$  track [value in radian].
- PhiMatchTol = 0.15** Tolerance in  $\phi$  for extrapolated tracks to match clusters; defined as  $(\text{PhiMatchTol} * \Delta z / 60)^2$ , where  $\Delta z$  is the distance to the previous cluster in  $z$ .
- PhiFirstTol = 0.05** Tolerance in  $\phi$  for first cluster in  $\phi$  list.
- AdjacentSectors = false** Turn off the search for clusters crossing  $RZ$  sectors.



## A.2 Pilot run/open tune of the code

The options for the open tune of the VELO are changes to the search windows and looking in the adjacent RZ sectors. The options to search for tracks crossing sectors was only added in PatVelo v2r11. The file VeloOpenTracking.opts sets this and contains:

```
PatVeloRTracking.AdjacentSectors = true;  
PatVeloRTracking.rExtraTol = 28.;  
PatVeloRTracking.rMatchTol = 7.2;  
  
ToolSvc.PatVeloSpaceTool.PhiMatchTol = 0.90;  
ToolSvc.PatVeloSpaceTool.PhiFirstTol = 0.30;  
ToolSvc.PatVeloSpaceTool.AdjacentSectors = true;
```

## References

- [1] “LHCb VELO Technical Design Report”, CERN-LHCC-2001-011
- [2] “LHC TDR - Yellow Book 1995”, EDMS 367815
- [3] “LHCb Technical proposal”, CERN-LHCC-98-004
- [4] “LHCb Reoptimised Detector”, CERN-LHCC-2003-030
- [5] “Study of resolution of VELO test-beam telescope”, LHCb-2000-103
- [6] “VELO raw data format and strip numbering”, EDMS 637676;  
“LHCb VELO and ST clusterisation on TELL1”, EDMS 690585
- [7] Olivier Callot, “Online Pattern Recognition”, CERN-LHCb-2004-094
- [8] Gauss 25r7, Boole v12r10, Brunel 30r14, XmlDDDB 30r14
- [9] Jeroen van Tilburg, “Track simulation and reconstruction in LHCb”, PhD thesis, 10/2005;  
Rutger van der Eijk, “Track reconstruction in the LHCb experiment”, PhD thesis, 9/2002
- [10] Rudolph Kalman, “A New Approach to Linear Filtering and Prediction Problems”, 1960 JBE **D82**, 35
- [11] Eduardo Rodrigues, “The LHCb Kalman Fit”, CERN-LHCb-2007-014
- [12] W.-M. Yao *et al.*, Journal of Physics **G 33**, 1 (2006)